Journal of Alloys and Compounds 509 (2011) 181–184

Contents lists available at ScienceDirect

Journal of Alloys and Compounds

journal homepage: www.elsevier.com/locate/jallcom

Particle size effect on the magnetic properties of NiO nanoparticles prepared by a precipitation method

K. Karthik[a,*], G. Kalai Selvan[a], M. Kanagaraj[b], S. Arumugam[b], N. Victor Jaya[a]

[a] Department of Physics, Anna University, Chennai 600 025, India
[b] Centre for High pressure Research, School of Physics, BARD, Tiruchirappalli 620 024, India

ARTICLE INFO

Article history:
Received 30 July 2010
Received in revised form 2 September 2010
Accepted 3 September 2010
Available online 16 September 2010

Keywords:
Nanoparticle
Precipitation
Magnetization
Exchange bias

ABSTRACT

Nickel oxide (NiO) nanoparticles of nominal size range 16 nm and 25 nm were obtained by controlling the calcination temperature. These particles were prepared by the precipitation method. Structural, optical and morphological characterizations were done by X-ray powder diffraction, UV–vis diffuse reflectance spectroscopy and scanning electron microscopy. Studies of magnetic measurements (up to 60 kOe) and temperature variations from 2 K to 300 K of the NiO nanoparticles were investigated. Particles of 16 nm exhibited a weak ferromagnetic component and hysteresis loop. There is a increase in coercivity H_c and the remanence M_r at 8 K accompanied by an exchange bias H_E. H_E monotonically tends to zero as the particles size varied from 16 nm to 25 nm. The hysteresis loop and the size dependent χ are interpreted with the uncompensated surface spins, whereas the transition at 30 K is suggested to be Néel temperature T_N of the spins in the core of the 16 nm particles. In addition, the increasing temperature cannot showed an approach to saturation in the magnetization curve, it indicates the possibility of an asperomagnetism and/or spin glass behavior of the NiO nanoparticles.

1. Introduction

Finite size effect of magnetism has become a very active area of research because of the unique properties of nanoscaled materials and their technological applications [1–3]. In nanoparticles, the surface spins dominate the magnetization due to their lower coordination and uncompensated exchange couplings. This is in turn leads to the changes in the magnetic properties [4–6]. However, the nanostructured oxides of antiferromagnet have very different magnetic natures as compared to the corresponding antiferromagnetic bulk materials [7]. Understanding the size dependent magnetization is not only important for practical applications; but also it is of great interest to identify the unprecedented nature of the antiferromagnetic oxide nanostructures between the structure and properties. Among many antiferromagnetic oxides, NiO has attracted much attention because of its high Néel temperature (523 K). Nanostructured NiO has been extensively studied in recent years because of its high magnetization and hysteresis loop shift after field cooling through the Néel temperature caused by the surface effect [8–10]. Tiwari and Rajeev proposed the detailed study on the NiO nanoparticles and stated the spin glass behavior originates by the surface spin disorder [11]. In addition, the exchange bias dominates the exchange coupling between the surface spins and the antiferromagnetic core leading to a shift of the magnetic hysteresis loop along the field axis [12]. In an antiferromagnetic nanoparticle, the fraction of surface to total spins depends on the particle size and hence the magnetic moment, coercivity and loop shift should vary with particle size [13–15]. Also, temperature dependent magnetic behavior of the surface spins leads to the enhanced magnetic moments, superparamagnetism, exchange bias and interparticle interaction [16–18].

In this paper, we report the synthesis of NiO nanoparticles by the novel precipitation method. Detailed magnetic investigations in the temperature range of 2–300 K and in magnetic fields up to 60 kOe were reported. Whereas, at lower temperature region (8 K) the particles exhibit a weak ferromagnetic component and hysteresis loop, it significantly showed a asperomagnetic behavior at 150 K and 300 K. For the 16 nm particle showed the significant exchange bias H_E (below at $T_N \approx 30$ K) with an enhanced coercivity value ($H_c = 770$ Oe) and it tends weakly towards zero as temperature increases to 300 K.

2. Experimental

2.1. Preparation of NiO nanoparticles

NiO nanoparticles were prepared through a novel precipitation method. Nickel(II) nitrate was used as a precursor for nickel. Aqueous oxalic acid was used as a solvent and polyethylene glycol was used for surfactant. The molar ratio of the precursor to the solvent ratio is (1:0.4) mol. The mixture was stirred at 2 h in

* Corresponding author. Tel.: +91 44 22358700; fax: +91 44 22358700.
E-mail address: karthik_kkdi@yahoo.com (K. Karthik).

0925-8388/$ – see front matter © 2010 Elsevier B.V. All rights reserved.
doi:10.1016/j.jallcom.2010.09.033

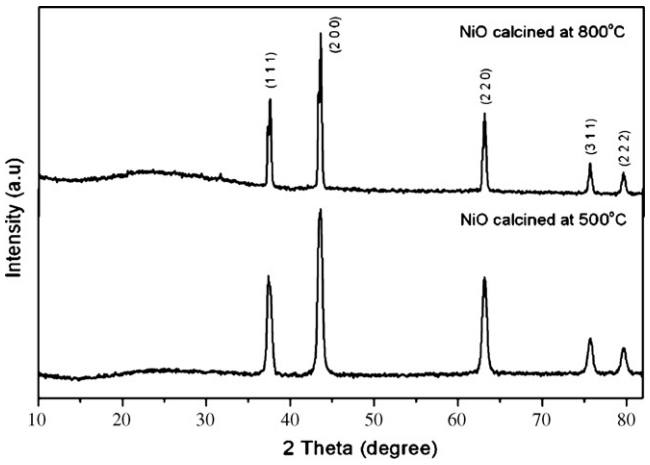

Fig. 1. X-ray powder diffraction plots of NiO nanoparticles.

room temperature. After stirring, the green precipitates were found. The precipitates were collected and washed several times with ethanol and water separately. The final product was maintained in an oven at 60 °C for the removal of hydroxyl radicals. The resultant NiO nanoparticle was further treated with an appropriate calcination temperature to obtain the better quality NiO nanocrystallites.

2.2.. Characterization and measurements

The structures of the samples were identified by X-ray powder diffraction (XRD) at room temperature on a PANalytical X'pert PRO X-ray diffractometer using Cu Kα radiation (λ = 1.5406 Å) as the X-ray source. The morphology and particle size of the prepared sample was examined by scanning electron microscopy (Hitachi S-3400). UV–vis absorption spectra of the prepared samples were recorded using UV–vis spectrophotometer (Shimadzu UV2401 PC). The magnetic properties of the NiO nanoparticles were studied by using a 9T Physical Property Measurement System (PPMS – Vibrating Sample Magnetometer of Quantum Design) in the temperature range of 2–300 K.

3. Results and discussion

3.1. Structural and morphological characteristics

The X-ray powder diffraction patterns of the calcined samples (Fig. 1) show only peaks due to NiO. Samples can be clearly indexed to a cubic structure (JCPDS # 73-1519), Fm-3m space group, without any observable peaks of impurity phases. Employing the Scherrerĭs relation [19], the average particle size is determined from the major peaks of the reflections. The average particles size (d) increases monotonously from 16 nm to 25 nm as the calcination temperature increases from 500 °C to 800 °C. It shows that the NiO nanoparticles are smaller at lower calcination temperature and we also found that, all diffraction peaks in Fig. 1 for the cubic structured NiO had a small but systematic shift toward higher angles with decreasing particle size was determined. The lattice parameters estimated from the XRD patterns are 4.167 Å and 4.163 Å respectively for the 25 nm and 16 nm particles, reflecting a slight decrease in the lattice parameters with the decrease in particle size. A lattice contraction with decreasing particle size seems reasonable from a thermodynamic point of view due to the higher surface curvature as is observed in many nanocrystalline materials [20]. It is apparent that the surface stresses and surface defect dipoles are the two phenomena governing the changes in the lattice volume as the particle size is reduced [21,22].

Typical SEM images of NiO nanoparticles are shown in Fig. 2. These images reveal a systematic evaluation of morphology of the prepared sample. It is observed from that the sample calcined at 500 °C shows homogeneous spherical shaped particles. The magnified image reveals that the average size of the particles is less than 25 nm.

3.2. Optical properties

UV–vis absorption spectroscopy is one of the important method to reveal the energy structures and optical properties of semiconductor nanocrystals. In our measurements, the sample was analyzed through the diffuse reflectance arrangement. The optical absorption spectrum of the NiO nanoparticles calcined at 500 °C is shown in Fig. 3. It is observed from that the strong absorption peak with broader shoulder could be detected in the wavelength range of 350–450 nm. The extrapolated value (the straight line to the x axis) gives the absorption energy corresponding to E_g = 2.93 eV. This increase in the band gap of the NiO nanoparticles is indicative of the quantum confinement effect arising from the tiny crystallites.

3.3. Magnetic properties

The temperature variation of magnetic susceptibility $\chi = M/H$ (H = 1.25 T) is plotted in Fig. 4 for 16 nm and 25 nm particles. Comparison of the behavior of χ versus T for the larger particle gives enhanced magnetic susceptibility plot as compared to the smaller particles. The small rise in χ seen at lower temperature region (below at 30 K) is observed and there is no evidence of any peaks. When a stronger magnetic field is applied (H = 1.25 T), the magnetization direction of the nanomaterials becomes easier and the blocking temperature T_B systematically decreases results the absence of peaks. However, the T_B should increase with increasing

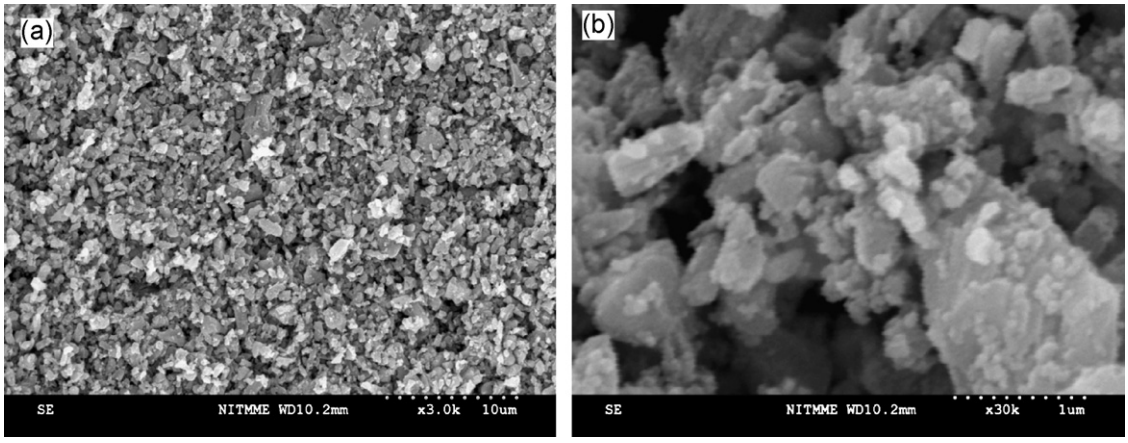

Fig. 2. SEM images of NiO nanoparticles calcined at 500 °C.

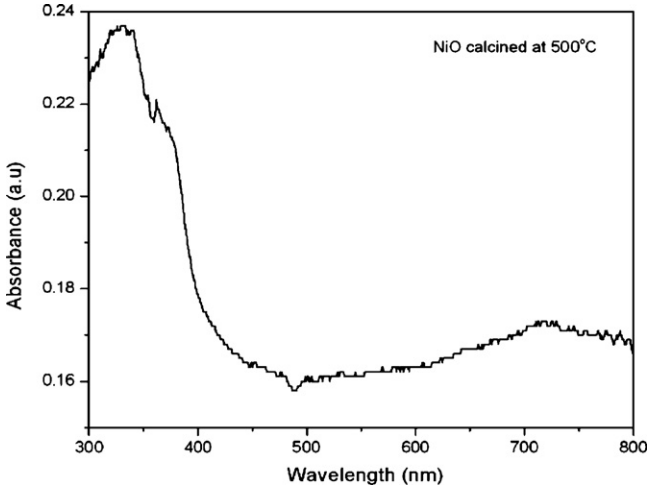

Fig. 3. UV–vis optical absorption spectrum of 16 nm NiO particles.

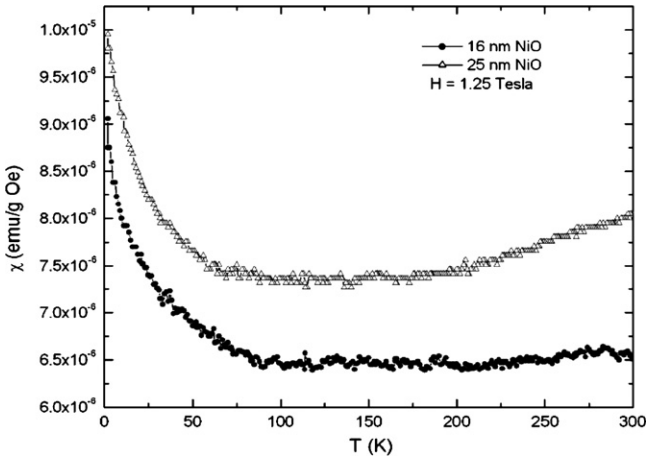

Fig. 4. Temperature variation of the magnetic susceptibility χ for different particle sizes.

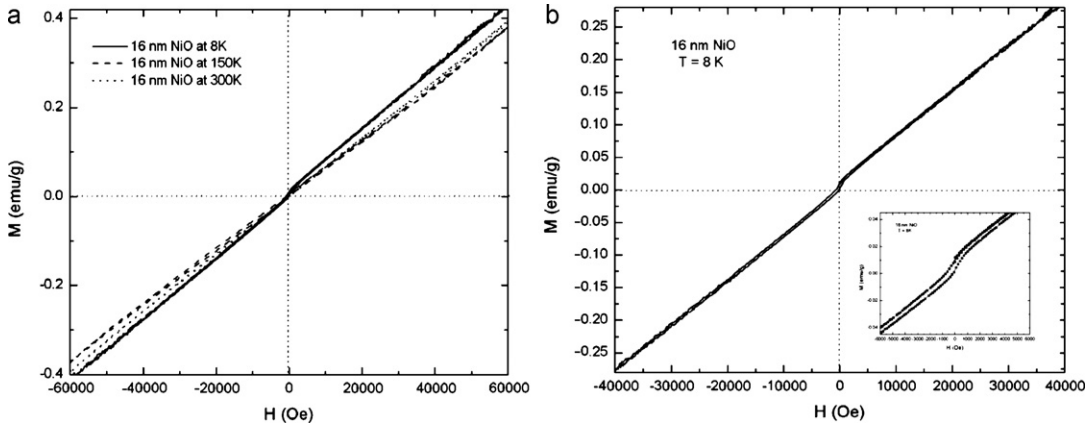

Fig. 5. (a) Measured magnetization of the 16 nm NiO nanoparticles as a function of applied field H up to 60 kOe at selected temperatures between 8 and 300 K and (b) the separate *M* versus *H* plot of 16 nm particles at 8 K and the inset shows the representation of H_{EB}.

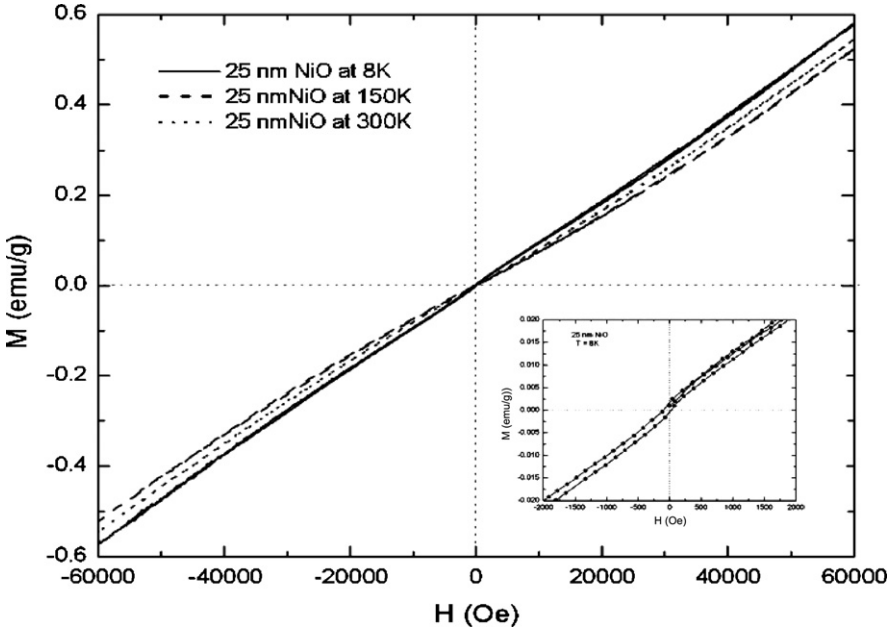

Fig. 6. The magnetization curves of the 25 nm NiO nanoparticles with the filed up to 60 kOe at selected temperatures between 8 and 300 K and the inset shows the *M* versus plot at 8 K.

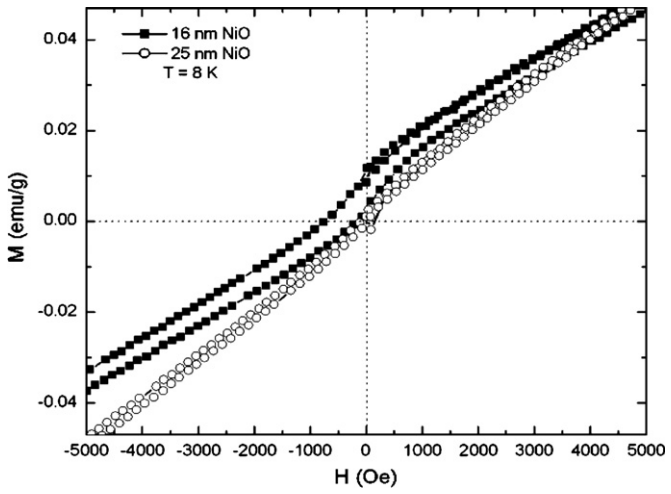

Fig. 7. Comparison of the hysteresis loop for the NiO nanoparticles as a function of particle size at 8 K.

particle size because the energy barrier separating the low energy states is proportional to the volume of the particles.

Uncompensated surface spins leads to the changes in the magnetic moment for $H \to 0$, which in turn greatly depends on the particle size, crystal structure and morphology of the particle. The measured magnetization under the maximum field of 60 kOe at temperatures ranges from 2 to 300 K are shown in Fig. 5a and b for the 16 nm particles. The plot shows the weak ferromagnetic component at 8 K in the lower field and it progressively exhibit a linear behavior up to 60 kOe. There is a dramatic increase in both M_r and H_c at 8 K for the 16 nm particles, mirroring the increase in χ observed in Fig. 4 below at 30 K. Both the M_r and H_c decreases slowly with the rise in temperature and at room temperature the magnetization value increases linearly with the applied field without the presence of hysteresis behavior. There is no sign of demagnetization plateau in the 16 nm particles for the magnetization curves at $T > 8$ K do not show an approach to saturation, it implies that the possibility of an asperomagnetism and/or spin glass behavior of the sample [9]. The inset of Fig. 5b for the low field region shows not only a shift H_E of the hysteresis loop to negative direction expected from exchange bias, but also the broadening of the loop ($H_c = 770$ Oe). It is anticipated that the exchange interaction between the surface spin layer and the antiferromagnetic core results the exchange bias [23].

Particles with $d > 16$ nm behave essentially as bulk NiO. The plots of M versus H at different temperatures between 2 and 300 K are shown in Fig. 6 for the 25 nm particles. The plots show essentially linear up to 60 kOe except for a weak ferromagnetic behavior at lower fields. The magnitude of the weak ferromagnetic component is much larger in the smaller particles as evident from the plots of M versus H for lower fields. We observe the weak ferromagnetic component originates at lower fields (8 K) only. The inset of Fig. 6 shows the weak ferromagnetic hysteresis loop shift to the positive direction expected the systematic shift in exchange bias ($H_E \to 0$) as the increase in particle size [15,24]. Indeed, the small particles have the larger interface area between the ferromagnetic phase and antiferromagnetic matrix. Thus the structural disorder and the exchange coupling strength are enhanced with the increase in interface area. As the particle size increases, the exchange interactions are weakened results the disappearance of H_{EB} as shown in Fig. 7. It is apparent that the coercivity value is very close to the ferromagnetic ordering at sufficiently small particle size. The observed H_c value for the 25 nm particle is 130 Oe and it infers that the H_c value decrease toward the increase in particle size. The magnetization curves for the particles at 150 K and 300 K show the linear dependence of the field. So the main conclusions from these investigations are that at $T \approx 30$ K and represents a transition to a magnetic state for which exchange bias is present.

4. Conclusions

The NiO nanocrystallites with different sizes were successfully synthesized by the precipitation method. We found that the particle size have strong influence on the magnetic properties of NiO nanoparticles. The measured magnetic susceptibility of NiO nanoparticles shows an approach to rise in behavior at lower fields (below at 30 K). The M versus H plot exhibits a weak ferromagnetic component at 8 K accompanied by an uncompensated surface spins. For the 16 nm particles, $T_N \approx 30$ K for the spins in the core is observed. Below this value (T_N), the exchange bias and the enhanced coercivity are observed. For particles greater than 16 nm, the weak ferromagnetic hysteresis loop shift to the positive direction expected the systematic shift in exchange bias. With an increase in temperature ($T > 8$ K), the magnetization curve cannot show an approach to weak ferromagnetic hysteresis and the magnetic ordering is essentially similar to the antiferromagnetic ordering. It indicates the possibility of an asperomagnetism and/or spin glass behavior of the NiO nanoparticles.

Acknowledgement

We acknowledge the DST Govt of India for providing PPMS-VSM at Bharathidasan University, Tiruchirappalli by which magnetic measurements were carried out.

References

[1] D.E. Speliotis, J. Magn. Magn. Mater. 193 (1999) 29.
[2] H.L. Huang, J.J. Lu, Appl. Phys. Lett. 75 (1999) 710.
[3] V. Skumryev, S. Stoyanov, Y. Zhang, G. Hadjipanayis, D. Givord, J. Nogues, Nature 423 (2003) 850.
[4] M.A. Morales, R. Skomski, S. Fritz, G. Shelburne, J.E. Shield, M. Yin, S. O'Brien, D.L. Leslie-Pelecky, Phys. Rev. B 75 (2007) 134423.
[5] R.H. Kodama, A.E. Berkowitz, Phys. Rev. B 59 (1999) 6321.
[6] X.H. Liu, W. Liu, X.K. Lv, F. Yang, X. Wei, Z.D. Zhang, D.J. Sellmyer, J. App. Phys. 107 (2010) 083919.
[7] S. Mørup, D.E. Madsen, C. Frandsen, C.R.H. Bahl, M.F. Hansen, J. Phys. Condens. Matter 19 (2007) 213202.
[8] S.A. Makhlouf, F.T. Parker, F.E. Spada, A.E. Berkowitz, J. Appl. Phys. 81 (1997) 5561.
[9] J.B. Yi, J. Ding, Y.P. Feng, G.W. Peng, G.M. Chow, Y. Kawazoe, B.H. Liu, J.H. Yin, S. Thongmee, Phys. Rev. B 76 (2007) 224402.
[10] R.H. Kodama, S.A. Makhlouf, A.E. Berkowitz, Phys. Rev. Lett. 79 (1997) 1393.
[11] S.D. Tiwari, K.P. Rajeev, Phys. Rev. B 72 (2005) 104433.
[12] W.H. Meiklejohn, C.P. Bean, Phys. Rev. 105 (1957) 904.
[13] S.A. Makhlouf, H. Al-Attar, R.H. Kodama, Solid-State Commun. 145 (2008) 1.
[14] K.O. Grady, L.E. Fernandez-Outon, G. Vallejo-Fernandez, J. Magn. Magn. Mater. 322 (2010) 883.
[15] M.S. Seehra, A. Punnoose, Solid-State Commun. 128 (2003) 299.
[16] J. Cohen, K.M. Creer, R. Pauthenet, K. Srivastava, J. Phys. Soc. Jpn. 17 (1962) 685.
[17] C.A. Mulder, A.J. van Duyneveldt, J.A. Mydosh, Phys. Rev. B 23 (1981) 1384.
[18] J.T. Richardson, D.I. Yiagas, B. Turk, K. Forster, M.V. Twigg, J. Appl. Phys. 70 (1991) 6977.
[19] B. Cullity, Elements of X-ray Diffraction, Addision-Wesley, Reading, MA, 1987, p. 294.
[20] J.Y. Zhang, X.Y. Wang, M. Xiao, Appl. Phys. Lett. 81 (2002) 2076.
[21] G. Li, J.B. Goates, B.F. Woodfield, L. Li, Appl. Phys. Lett. 85 (2004) 2059.
[22] S. Tsunekawa, K. Ishikawa, Z.Q. Li, Y. Kawazoe, A. Kasuya, Phys. Rev. Lett. 85 (2000) 3440.
[23] J. Nogues, J. Sort, V. Langlais, V. Skumryev, S. Suriñach, J.S. Munoz, M.D. Baro, Phys. Rep. 422 (2005) 65.
[24] S.Y. Yin, S.L. Yuan, Z.M. Tian, L. Liu, C.H. Wang, X.F. Zheng, H.N. Duan, S.X. Huo, J. Appl. Phys. 107 (2010) 043909.